Biomedical Signal Processing and Control 81 (2023) 104499



Contents lists available at ScienceDirect

Biomedical Signal Processing and Control

journal homepage: www.elsevier.com/locate/bspc

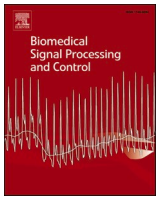



COVID-19 and human development: An approach for classification of HDI with deep CNN

Gürkan Kavuran [a,*], Şeyma Gökhan [b], Celaleddin Yeroğlu [c]

[a] Department of Electrical and Electronics Engineering, Faculty of Engineering and Natural Sciences, Malatya Turgut Ozal University, Malatya, Turkey
[b] TUBITAK BILGEM Software Test and Quality Evaluation Laboratory, Turkey
[c] Department of Computer Engineering, Faculty of Engineering, Inonu University, Malatya, Turkey

ARTICLE INFO

Keywords:
Human Development Index
Deep learning
COVID-19
Continuous wavelet transform
Artificial intelligence
Classification

ABSTRACT

The measures taken during the pandemic have had lasting effects on people's lives and perceptions of the ability of national and multilateral institutions to drive human development. Policies that changed people's behavior were at the heart of containing the spread of the virus. As a result, it has become a systemic human development crisis affecting health, the economy, education, social life, and accumulated gains. This study shows how the relationship of the Human Development Index (HDI), which has combined effects on health, education, and the economy, should be considered in the context of pandemic factors. First, COVID-19 data of the countries received from a public and credible source were extracted and organized into an acceptable structure. Then, we applied statistical feature selection to determine which variables are closely related to HDI and enabled the Deep Convolutional Neural Network (DCNN) model to give more accurate results. The Continuous Wavelet Transform (CWT) and scalogram methods were used for the time-series data visualization. Three different images of each country are combined into a single image to penetrate each other for ease of processing. These images were made suitable for the input of the ResNet-50 network, which is a pre-trained DCNN model, by going through various preprocessing processes. After the training and validation processes, the feature vectors in the fc1000 layer of the network were drawn and given to the Support Vector Machine Classifier (SVMC) input. We achieved total performance metrics of specificity (88.2%), sensitivity (96.5%), precision (99%), F1 Score (94.9%) and MCC (85.9%).

1. Introduction

The disease called COVID-19, caused by the new type of coronavirus that emerged in Wuhan, China, has adversely affected the world in many ways. A pandemic was declared by the World Health Organization (WHO) on March 11, 2020. As of December 1, 2021, the total number of cases worldwide was 262 million 178 thousand 403, while the total deaths were 5 million 215 thousand 745. Turkey ranks sixth in the world with 8 million 795 thousand 588 cases. While the first dose of vaccine was administered to 56 million 38 thousand 139 people, the second dose was administered to 50 million 750 thousand 190 people. Turkey became the 6th country with the highest number of vaccinations after the United States of America, India, and Brazil [1,2,3].

It has been clearly stated that the COVID-19 pandemic is more than a health emergency faced and is a systemic crisis affecting the world economy [4]. In many parts of the world, the pandemic is causing a crisis in human development. Today's conditions are comparable to deprivation levels last observed in the mid-1980 s in some dimensions of human development. However, the crisis is having a significant impact on all aspects of human growth, including income, health, and education. Although it is known that the pandemic has indirect effects on the increasing gender-based violence, it has not yet been thoroughly documented. Human capital is a critical driver of long-term prosperity, poverty reduction, and prosperous societies [5]. It should be connected with education and training and all types of activities that boost labor productivity and raise future income levels. In this regard, health-related expenditures are also seen as human capital investments [6]. Models made utilizing artificial intelligence began to make early diagnosis and treatment of patients easier at the outset of these investments.

The fact that the studies on artificial intelligence (AI) are applicable in many fields of science today is an indication that it has a practical and robust theoretical background [7,8]. AI can assist us in combating this

* Corresponding author.
E-mail address: gurkan.kavuran@ozal.edu.tr (G. Kavuran).

https://doi.org/10.1016/j.bspc.2022.104499
Received 21 April 2022; Received in revised form 18 October 2022; Accepted 1 December 2022
Available online 12 December 2022
1746-8094/© 2022 Elsevier Ltd. All rights reserved.

virus by recommending population screening, medical assistance, notification, and infection management [9]. In recent studies, the effectiveness of AI applications in the diagnosis of COVID-19 pneumonia has been investigated, and it has been determined to have great diagnostic performance in this field [10–14]. There are many studies in the literature about the combination of AI and medical applications related to COVID-19. For example, researchers at Mount Sinai have created an AI system to help diagnose COVID-19 patients using an algorithm trained on more than 900 Computed Tomography (CT) lung scans from Chinese patients [15]. Another AI system, developed by researchers at MIT, can detect COVID-19 based on the sound of a patient's coughing [16]. It has been shown that the DL-CRC model created using the DARI algorithm and the CNN model can be accurately detected by X-ray [17]. Using CNN and ConvLSTM as two deep learning methods, it has been shown that COVID-19 and normal cases can be tested on both CT and X-ray images. An efficient diagnosis can be made to detect COVID-19, among other related infections [18]. The CNN-based transfer learning-BiLSTM hybrid construct has been shown to be highly effective for diagnosing COVID-19. Since the proposed study automatically performs the segmentation process, it provides high classification accuracy and convenience [19]. Yang and colleagues analyzed 152 CT images using CNN and demonstrated an accuracy of 0.89 in diagnosing COVID-19 [20]. Ahamed et al. developed an extended ResNet50V2 based deep learning model where finetuning has been performed to detect and diagnose COVID-19 infected cases [21]. Kavuran et al. evaluated a fully automatic deep-learning system for the diagnosis of COVID-19 using thoracic computed tomography in [22]. They reached an overall accuracy of 97.7 % with the optimized features from concatenated layers.

Within the scope of this study, a machine learning-based decision support system has been proposed in order to find the relationship between the HDI of countries and the COVID-19 data of that country. These time-varying data basically include approximately 35 variables, such as the number of daily cases, the number of tests, the death rate, the vaccination rate, and sociodemographic information. First of all, statistical feature selection was applied to determine which of these variables are closely related to HDI and enable the DCNN model to give more accurate results. According to the ANOVA f-value, the study was started by considering the variable with the highest three scores for each country. For the visualization of the time series data, the Continuous Wavelet Transform (CWT) method and the scalogram method were used. Three different images of each country are combined into a single image to penetrate each other for ease of processing. These images were made suitable for the input of the ResNet-50 network, which is a pre-trained DCNN model, by going through various preprocessing processes. The weighting coefficients in the learnable convolution layer (fc1000) of the network have been revised, and the classification performance has been increased. After the training and validation processes, the feature vectors in the fc1000 layer of the network were drawn and given to the SVMC input, which is another machine learning-based classifier. Based on the confusion matrix and Receiver Operating Characteristic (ROC) curves, system performance was examined using metrics such as accuracy, sensitivity, specificity, sensitivity, F1, and Matthew Correlation Coefficient (MCC).

In the second part of the study, the steps of the proposed method will be explained. While the experimental results are given in Chapter 3, the results and discussion are given in Chapter 4.

2. Methodology

In this section, the steps of the proposed method will be explained in sub-headings. The study can be examined under three main topics. In the first stage, data cleaning processes were carried out by obtaining the publicly available data set. Thus, an operable form was created from the raw data. Since the number of features that make the data meaningful is high, elimination has been made. Attribute selection helps us remove the less important parts of the data and shorten the training time. For data labeling, the three selected attribute vectors were associated with the HDI of the related country. The "new_tests" vector, which is the third component of the obtained package, was scanned according to the sliding window method with a length of 50 units, and its standard deviation was taken. Inner Penetrated Images (IPI) were created by composing three separate scalogram images into each other for each class. Thus, a single image containing the structural features of all three images was obtained. In the next stage, the pre-trained ResNet-50 network, which is used as a deep convolutional neural network, was fed with the obtained IPI images. During the learning period, the number of images was increased at this step by using image augmentation methods online. The feature vectors from the modified fc1000 fully connected layer of the ResNet-50 were normalized to zero mean to be given to the SVMC input. In the last stage, deep feature vectors drawn from the trained network are reserved for 75 % training and 25 % validation. Evaluation metrics are presented with the help of the ROC curve and complexity matrix. The schematic diagram of the study is given in Fig. 1.

2.1. Preprocess data for domain-specific deep learning

2.1.1. Data description and feature selection

The dataset used in this study was obtained by reporting data on confirmed cases and deaths, managed by a team at the Johns Hopkins University Center for Systems Science and Engineering (CSSE). Since January 22, 2020, data on confirmed cases and deaths for all countries has been updated several times daily. This data is obtained from national and local agencies of governments, and a complete list of data sources for each country is published on the Johns Hopkins GitHub site [23]. Fig. 2. shows cumulative confirmed cases of COVID-19 as of January 11, 2022. The number of confirmed cases is lower than the actual number of infections due to limited testing.

In the dataset consisting of a total of 187 countries, we have taken the time-dependent changes between February 14, 2020, and August 10, 2021, given in Table 2. These form the predictors' vectors that we will use in the study. We chose HDI as the output vector in order to classify the relationship of the feature vectors of each country with the HDI, which is a metric that measures how far people have come in their development in three fundamental characteristics of humans: living a long and healthy life, having access to knowledge, and having a reasonable quality of living. The HDI is calculated as the geometric mean of the three-dimensional index [24],

$$HDI = \left(I_{Health} \cdot I_{Education} \cdot I_{Income}\right)^{1/3} \tag{1}$$

In the 2014 Human Development Report, a system of predetermined cutoff criteria for the four categories of human development accomplishments was implemented. This Report retains the same HDI cutoff parameters for categorizing nations announced in the 2014 Report as in Table 1.

Thus, we aimed to reveal the structure of the link between COVID-19 data and HDI. The unstable change and instability in COVID-19 data do not constitute a clear boundary between countries in terms of HDI. Therefore, M and L classes are grouped under L, and H and VH classes are under H. We eliminated some of the 35 predictor vectors considered using the univariate feature selection method for the deep CNN structure to give more accurate results.

When preparing a big dataset for training, selecting the best features is critical. It assists us in removing less essential sections of the data and reducing training time. It can be viewed as a phase in deep CNN preprocessing. Univariate feature selection chooses the best features based on statistical testing. To expose feature selection routines, we used Python Scikit-learn modules. For the samples in Table 1, we compute the ANOVA F-value [25]. The modules remove all but the highest-scoring features. These objects accept a scoring function as an input and return univariate scores and p-values. This method can be used on sample sets for feature selection and dimensionality reduction to either increase

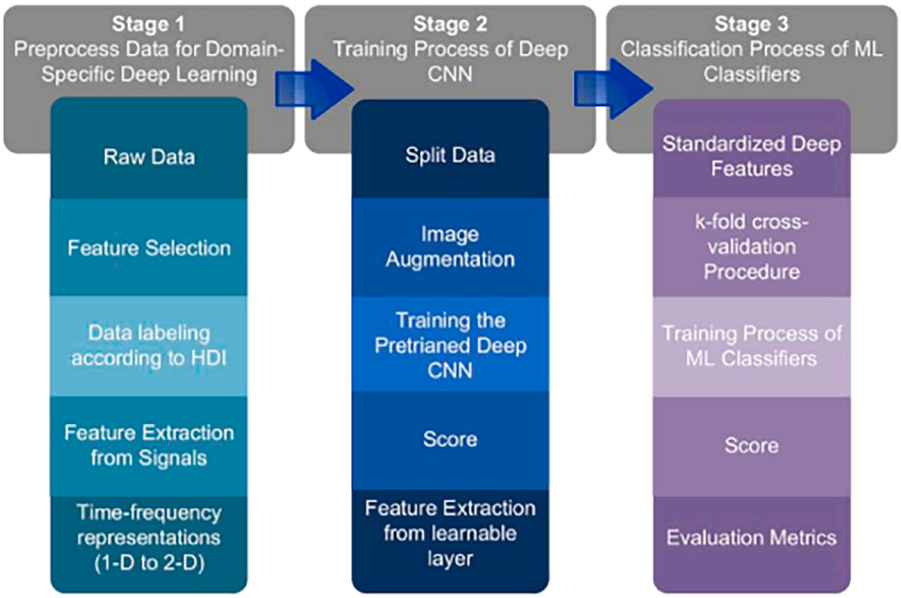

Fig. 1. Schematic diagram of the study.

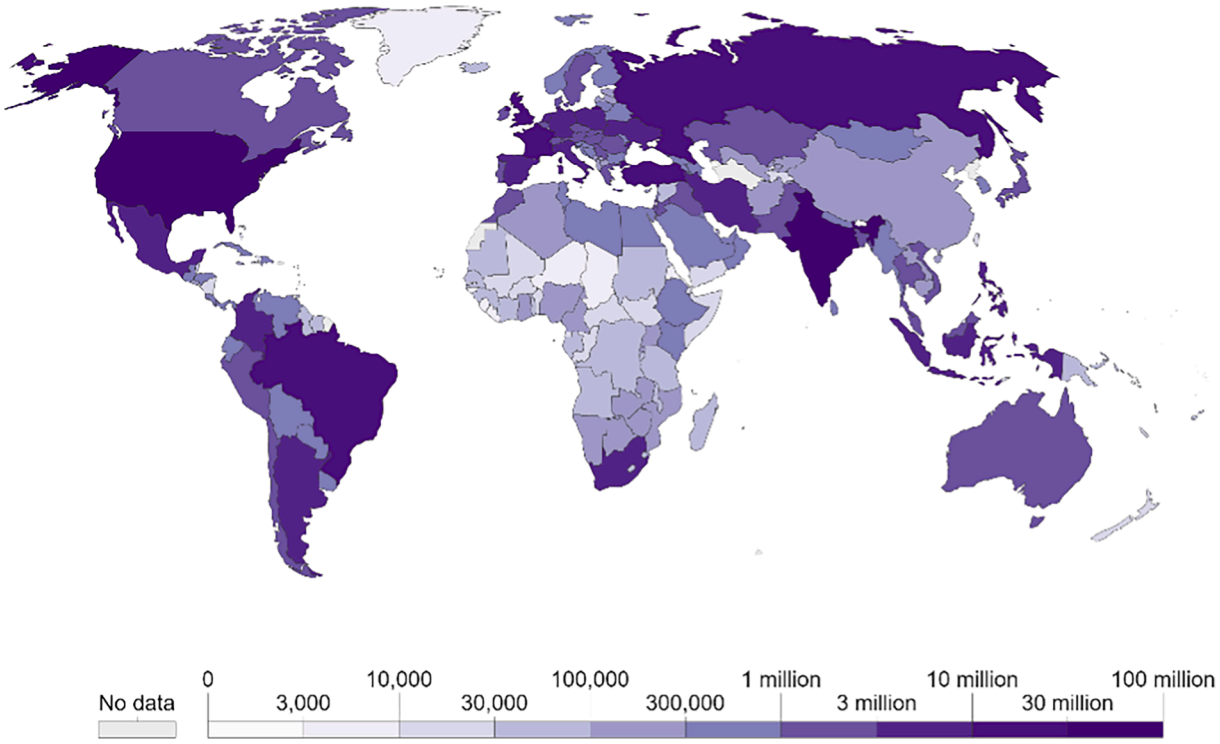

Fig. 2. Cumulative confirmed COVID-19 cases, January 11, 2022 [23].

Table 1
Cutoff points on the HDI for grouping countries [24].

Very high human development (VH)	0.800 and above
High human development (H)	0.700–0.799
Medium human development (M)	0.550–0.699
Low human development (L)	Below 0.550

deep CNN accuracy scores or improve their performance on very high-dimensional datasets. It provides the optimal class for extracting the most useful features from a given dataset. This technique chooses the features based on the k highest score. The method can be used with both classification and regression data. The feature importance graph is given in Fig. 3. The top 4 feature vectors with the best score are ID_26 (new tests smoothed), ID_22 (new tests), ID_4 (total deaths), and ID_1 (total cases), respectively. One of these two vectors was chosen since ID_26 is a smoothed version of ID_22. In comparison to raw data, smoothed data eliminates reporting irregularities and provides a more accurate view of time. Data at the state level is noisy at the raw data level, making it challenging to detect trends. Thus, a feature vector package with an average length of 3x550 for each country was obtained.

It is necessary to highlight some features in the signal structure that

Table 2
List of the predictors for COVID-19.

ID	Predictors	ID	Predictors
1.	Total cases	**19.**	Weekly icu admissions per million
2.	New cases	**20.**	Weekly hospital admissions
3.	New cases smoothed	**21.**	Weekly hospital admissions per million
4.	Total deaths	**22.**	New tests
5.	New deaths	**23.**	Total tests
6.	New deaths smoothed	**24.**	Total tests per thousand
7.	Total cases per million	**25.**	New tests per thousand
8.	New cases per million	**26.**	New tests smoothed
9.	New cases smoothed per million	**27.**	New tests smoothed per thousand
10.	Total deaths per million	**28.**	Positive rate
11.	New deaths per million	**29.**	Tests per case
12.	New deaths smoothed per million	**30.**	Tests units
13.	Reproduction rate	**31.**	Total vaccinations
14.	Icu patients	**32.**	People vaccinated
15.	Icu patients per million	**33.**	People fully vaccinated
16.	Hosp patients	**34.**	New vaccinations
17.	Hosp patients per million	**35.**	New vaccinations smoothed
18.	Weekly icu admissions		

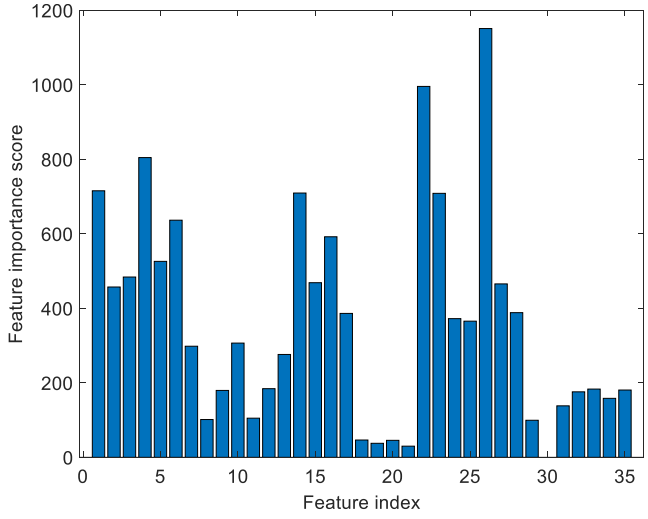

Fig. 3. Feature importance graph.

changes depending on time. This situation provides positive benefits in the performance of the classifier [26,27]. Some statistical methods are available for the analysis and interpretation of these properties. In order to choose the appropriate statistical method for data analysis, it is necessary to know the assumptions and conditions of statistical methods. One of these methods is the standard deviation. The standard deviation is a statistical analysis approach for determining the spread of data around the mean. When dealing with a high standard deviation, this refers to data that is spread out from the mean over a vast area. Similarly, a low deviation shows that most data agree with the mean and can also be referred to as a cluster's expected value. The standard deviation is mostly used to determine the distribution of data points. The "new_tests" vector, which is the third component of the obtained data package, was scanned according to the sliding window method with a length of 50 units, and its standard deviation was taken. The formulation of the standard deviation is given in Equation (2).

$$Standard = \left(\frac{1}{N-1}\sum_{i=1}^{N}\left(X(i)-\overline{X}\right)^2\right)^{\frac{1}{2}} \tag{2}$$

Time-Frequency Representations.

In many engineering applications, time–frequency analysis is an effective tool for the in-depth investigation of signal properties, separating input signals into their time-varying spectral components. The Continuous Wavelet Transform (CWT) has played an essential role in analyzing time–frequency data. This section will discuss the CWT method for 2D time–frequency representation of time series COVID-19 data. CWT is a method that allows us to analyze time scale features (new tests, total deaths, total cases) in COVID-19 data at different times and scales. The timescale feature in CWT allows obtaining high time–frequency resolution, which helps identify sub-features of COVID-19 data. Wavelet analysis is commonly used to extract local characteristics, as it can provide an in-depth perspective of the temporal and frequency fluctuation of the examined signals. The CWT of time series COVID-19 data is represented as:

$$C(a,b,f(t),\psi(t)) = \frac{1}{\sqrt{a}}\int_{-\infty}^{\infty} f(t)\psi^{*}\left(\frac{t-b}{a}\right)\cdot dt \tag{3}$$

where, ψ(t) is the mother wavelet, a is the scale, $C(a,b)$ is the CWT coefficients, and b is the time shift. Deviations of cumulative total cases, cumulative total deaths, and daily new COVID-19 tests against to days for Albania and the Democratic Republic of Congo are given in Fig. 4.

The scalogram aids in visualizing rapid changes in the signal by utilizing the coefficients acquired after applying the continuous wavelet transform to the signal. The CWT scalogram is a two-dimensional drawing that depicts time on the horizontal axis and scales on the vertical axis. Fig. 5 illustrates the scalogram of ID_22 (new tests), ID_4 (total deaths), and ID_1 (total cases) for both High HDI and Low HDI classes. The time–frequency representations of the scalograms are sent into the input of deep CNN structures that will be utilized to classify. Filter banks contribute to the extraction of frequency content by passing scalogram images obtained with COVID-19 data through various filters. IPI were created by composing three separate images into each other for each class to eliminate the processing complexity and make the training-validation data distribution correctly. Thus, a single image containing the structural features of all three images was obtained. Fig. 4 depicts the scalogram and IPI images of High-Low HDI.

2.2. Deep CNN and SVM model

This section presents the methodological content of the proposed method. Deep learning is a method of developing mathematical models using artificial intelligence without predetermining the signal or image attributes. Throughout reality, neural networks automatically extract and define features in the deep learning process. The output of each previous layer is sent as input to the next layer, and then events "L" or "H" are formed. Hidden layers process significant qualities, which are subsequently supplied to each of the deep levels. Fig. 6 shows the Resnet-50 structure, with input features traveling through 50 hidden layers before reaching the modified fully connected layer and SVMC, which are classed as "L" or "H."

CNN is one of the systematic structures used in deep learning algorithms that is successful on huge data. A ResNet-50 model is adopted in this research, which is a pre-trained CNN network with 1000 categories and over one million images [6]. ResNet-50 will be trained to identify a new set of IPI photos and detect HDI using the IPI images collected in the previous section. An input layer, 50 deep layers (convolution layers, bulk normalization layers, and ReLU), classification layers (average pooling layers, fully connected layers, and SoftMax layers), and output layers comprise ResNet-50. Input images have been resized to 224x224 pixels to be compatible with ResNet-50 models.

During the learning phase, the number of data was expanded by using online image augmentation technologies to minimize imbalance and overfitting issues in the number of images for each class. A compelling image classifier was designed using MATLAB's image data augmentation module. This paper proposes a two-stage classification process: feature extraction using pre-trained deep network structures and labeling of IPI images using SVMC [28–30]. Deep CNN features were

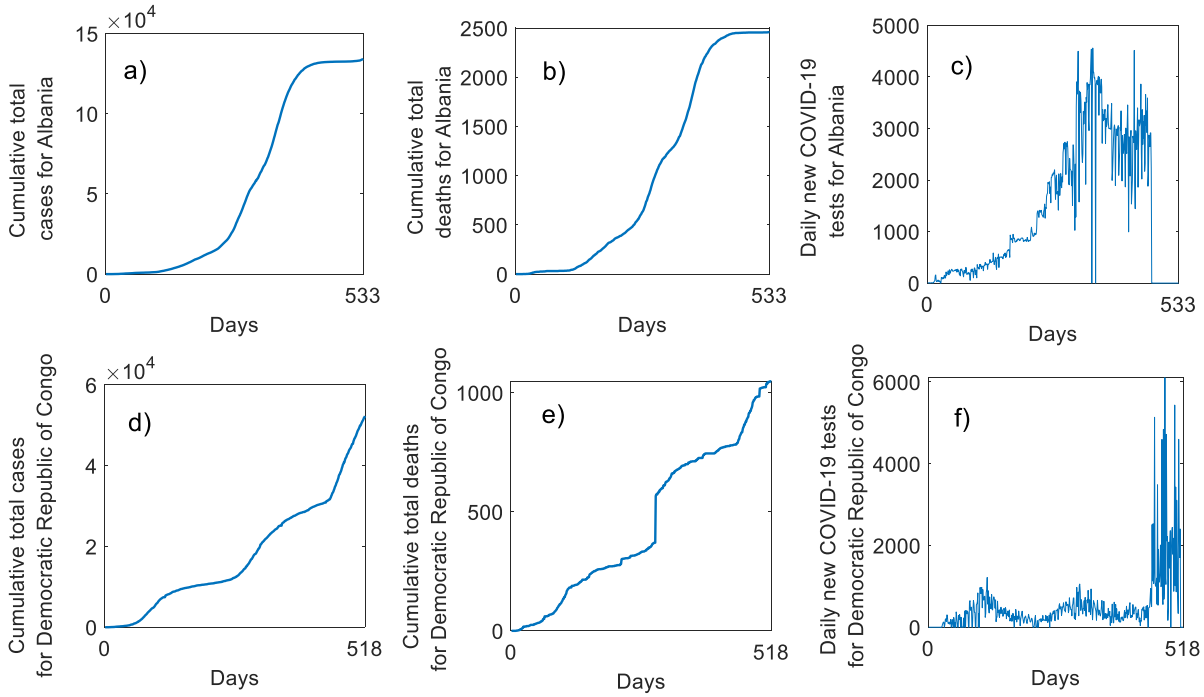

Fig. 4. Deviation of cumulative total cases, cumulative total deaths, and daily new COVID-19 tests against days for Albania and the Democratic Republic of Congo.

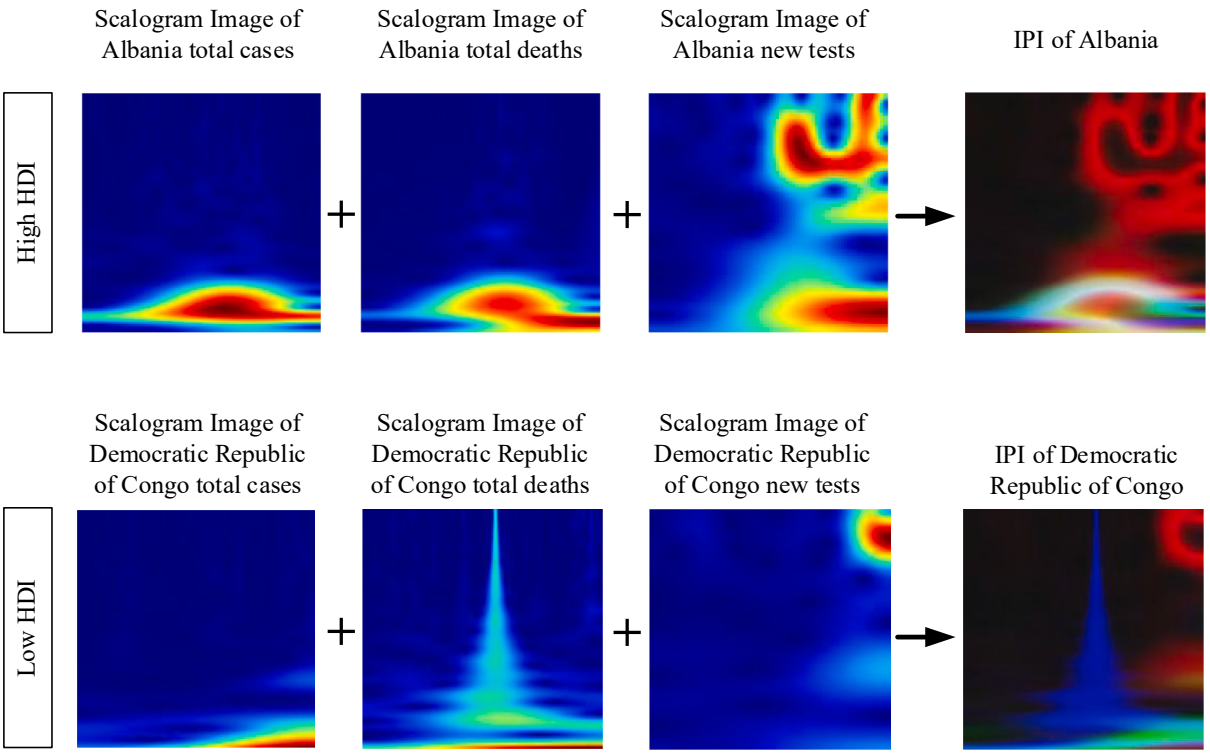

Fig. 5. An example of Scalogram and IPI images of High-Low HDI.

retrieved from ResNet-50 activations using modified fc1000 activations. The mean of all feature sets was adjusted to zero. In the classification phase, SVMC was employed with 75 percent training and 25 percent test data. The proposed method's validity and its impact on the evaluation criteria are presented concerning computing efficiency. All the experiments were performed in a MATLAB environment running on a PC with AMD Ryzen 5 2600 3.4 GHz CPU, 64 GB memory, and 12 GB NVIDIA GeForce RTX 2080 TI GPU.

3. Experimental results

The performance of the suggested design will be analyzed in this section using statistical assessment criteria. Accuracy (ACC), Sensitivity (Sens.), Specificity (Spec.), Precision (Prec.), F1 score (F1), and MCC

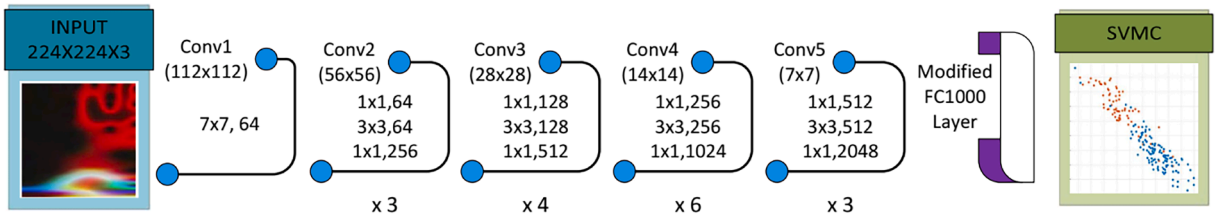

Fig. 6. ResNet-50 architecture.

were all calculated using the confusion matrix. The expected and actual classes are represented by rows and columns in the confusion matrix. Correctly categorized observations are denoted by crossover cells, whereas erroneously classified observations are represented by other cells. Each cell contains the number of observations as well as the percentage of the overall number of observations. The percentages of all samples projected to belong to each class categorized true (precision measures) and false are shown in the graph's far-right column (false discovery rate measures). The cell in the matrix's lower right corner represents total accuracy. The ROC curve, which shows the true positive rate as a function of the false positive rate, is also one of the most extensively used metrics for evaluating the effectiveness of machine learning algorithms. Equation 4–9 defines the evaluation metrics that were used.

$$Accuracy = \frac{N_{TP} + N_{TN}}{N_{TP} + N_{TN} + N_{FP} + N_{FN}} \tag{4}$$

$$Sensitivity = \frac{N_{TP}}{N_{TP} + N_{FN}} \tag{5}$$

$$Specificity = \frac{N_{TN}}{N_{TN} + N_{FP}} \tag{6}$$

$$Precision = \frac{N_{TP}}{N_{TP} + N_{FP}} \tag{7}$$

$$F_1 = \frac{2N_{TP}}{2N_{TP} + N_{FP} + N_{FN}} \tag{8}$$

$$MCC = \frac{N_{TP}N_{TN} - N_{FP}N_{FN}}{\sqrt{(N_{TP} + N_{FP})(N_{TP} + N_{FN})(N_{TN} + N_{FP})(N_{TN} + N_{FN})}} \tag{9}$$

Here, N_{TP}, N_{TN}, N_{FP}, and N_{FN} define the number of true-positive classes, the number of true-negative classes, the number of false-positive classes, and the number of false-negative classes, respectively. The SVMC's multi-class confusion matrix, which was fed by the deep feature set, is shown in Fig. 7a. There are three misclassified samples among the 46 validation samples, according to the confusion matrix. With two samples, the "L" class was determined to have the most misclassified samples. The ROC curves of the predicted classes with AUC values are given in Fig. 7b. The area of the ROC curve was obtained as 0.961 and 0.969 for "L" and "H" classes, respectively.

The SVMC's general classification scores are listed in Table 3. The total metric values for the COVID-19 dataset were observed in the proposed design with 187x2 features, as shown in the table. For the COVID-19 dataset, the model utilizing deep features from the updated fc1000 layer had an overall accuracy of 93.4 percent. The remaining overall performance indicators, Spec., Sens., Prec., F1, and MCC, scored 88.2 %, 96.5 percent, 99 percent, 94.9 percent, and 85.9 %, respectively.

4. Conclusion

Artificial intelligence has revolutionized diagnostic imaging systems and is one of the trendiest subjects in medical imaging. Deep learning approaches, particularly the usage of CNNs, have resulted in significant performance improvements over traditional machine learning techniques. The importance of non-medical data becoming clinical predictors has been extensively reviewed in the literature. This study is based on medical data and demonstrates the correlation between HDI calculated using socioeconomic inputs. To the best knowledge of the authors, this paper is the first that uses signal processing techniques with DCNN for the classification of HDI by using COVID-19 data. According to this study, HDI, which has integrated effects on health, education, and the economy, should be addressed in the context of pandemic causes. First, COVID-19 data from the countries were retrieved and structured into an acceptable structure using information obtained from a public and reliable source. Then, using statistical feature selection, we figured

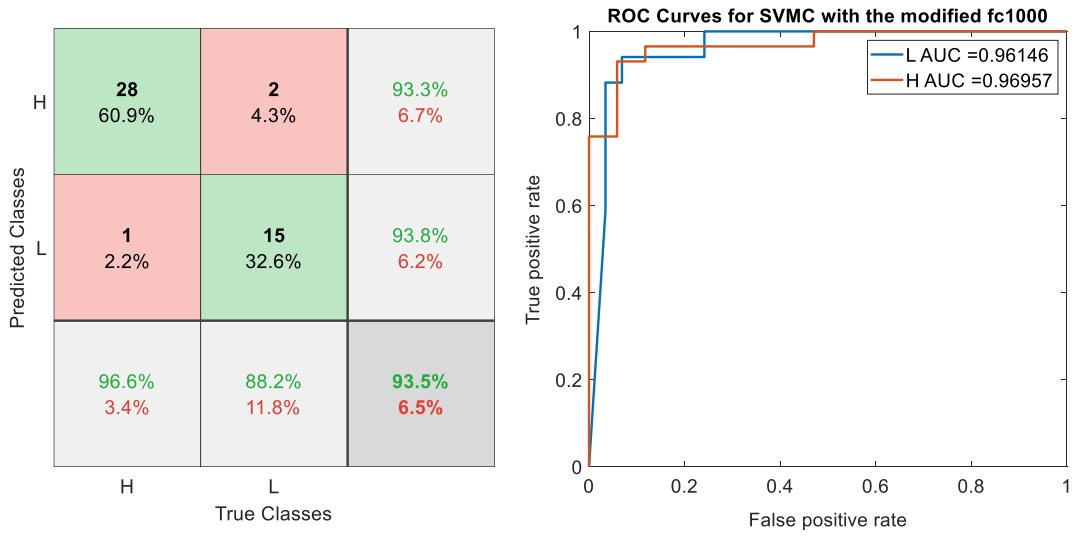

Fig. 7. a) The confusion matrix of the SVMC with deep features. b) The ROC curves of all classes for deep features.

Table 3
The general classification scores of the SVMC for the deep feature set.

	Evaluation Metrics					
	Accuracy	**Sensitivity**	**Specificity**	**Precision**	**F1**	**MCC**
Results	0.934	0.965	0.882	0.990	0.949	0.859

out which factors are closely associated with HDI, allowing the DCNN model to produce more accurate findings. The time-series data visualization was done using the CWT and scalogram methods. For the convenience of processing, three separate images of each country are merged into a single image to pierce each other. By going through different preprocessing steps, these images were made acceptable for the input of the ResNet-50 network, which is a pre-trained DCNN model. The feature vectors in the fc1000 layer of the network were created and given to the SVMC input after the training and validation operations. The complete performance parameters of specificity (88.2 %), sensitivity (96.5 %), accuracy (99 %), F1 Score (94.9 %), and MCC (85.9 %) were all achieved.

In this study, we found a significant correlation between the socioeconomic standing of a nation and the COVID-19 effects. Previous studies have demonstrated a substantial correlation between sociodemographic risk variables and COVID-19 incidence and mortality [31]. A lower percentage of COVID-19 vaccinations and fewer testing is linked to lower socioeconomic levels. It demonstrates how it has a negative impact on people's lives and increases the disease burden in low-income countries [32,33]. On the other hand, prior research demonstrates that the COVID-19 epidemic has both expanded and generated new socioeconomic inequalities [34].

Key elements for speeding vaccination coverage at the national level include socioeconomic variables and the health policies of the governments. Daily test rates are one of these issues. One of our most crucial tools in the effort to prevent and stop the spread of the virus and minimize its effects during the pandemic is daily testing. The tests enable us to locate and confine infected peoples' contacts. It can also help allocate medical resources and staff more efficiently. Therefore, the use of daily test data as the determining factor in this study played an important role in the classification of countries in terms of HDI. Examining the graphs in Fig. 4, it becomes clear that the variance in daily test numbers accounts for the majority of the differences between nations with high and low HDI. This circumstance is believed to have a favorable impact on classification performance.

There are several types of research in the literature about the association between HDI and confirmed COVID-19 cases by country. The hierarchical multiple linear regression models are presented in [35] to identify factors associated with confirmed cases of COVID-19 with a focus on the HDI. Countries with a high HDI could conduct more tests per person, leading to more confirmed cases than those with a low HDI. The Pearson correlation test and univariate linear regression analysis were performed on the relationship between HDI, HDI-Education Level, HDI-Life Expectancy, and HDI-Gross National Income per capita and COVID-19 deaths in Brazil [36]. Palamim et al. showed the case fatality rate depends on at least 20–40 % of the HDI. Ameye et al. proposed a method to assess the Case Fatality Rate (CFR) of COVID-19 as an indicator to evaluate Nigeria's performance relative to other selected countries based on the HDI using hierarchical clustering [37]. Generally, statistical analysis was used in the methodology of these studies. To the best of the authors' knowledge, similar research using the methods suggested in this study has not been found in the literature. It is thought that this study, which structurally includes signal processing, statistical analysis, feature selection, and deep learning methods, will contribute to the literature. The study, which provides for the network analysis showing the relationship between the selected features and the dependent variable, will be on our next agenda.

Funding

This study was funded by Inonu University Scientific Research Projects Management Unit with the project number FYL-2021-2377.

CRediT authorship contribution statement

Gürkan Kavuran: Conceptualization, Methodology, Data curation, Validation, Software, Formal analysis, Visualization, Writing – original draft. **Şeyma Gökhan:** Conceptualization, Methodology, Data curation. **Celaleddin Yeroğlu:** Writing – review & editing, Supervision, Project administration, Funding acquisition.

Declaration of Competing Interest

The authors declare the following financial interests/personal relationships which may be considered as potential competing interests: 'Celaleddin YEROGLU reports a relationship with Inonu University that includes: funding grants. This study was funded by Inonu University Scientific Research Projects Management Unit with the project number FYL-2021-2377.'

Data availability

Data will be made available on request.

References

[1] WHO, 2021. Available from: <Https://Www.Who.Int/Emergencies/Diseases/Novel-Coronavirus-2019/>.
[2] Department of Error: Nowcasting and forecasting the potential domestic and international spread of the 2019-nCoV outbreak originating in Wuhan, China: a modelling study (The Lancet (2020) 395(10225) (689–697), (S0140673620302609), (10.1016/S0140-6736(20)30260-9)), Lancet 395 (2020), doi: 10.1016/S0140-6736(20)30302-0.
[3] who.covid19, 2021. Available from: <Https://Covid19.Who.Int/>.
[4] www.un.org/en/coronavirus/UN-response, Https://Www.Un.Org/En/Coronavirus/UN-Response. (n.d.).
[5] WorldBank, The Human Capital Index 2020 Update Human Capital in the Time of Covid-19, International Bank for Reconstruction and Development / The World Bank, 2020.
[6] J.A. Hasnaoui, S.K.A. Rizvi, K. Reddy, N. Mirza, B. Naqvi, Human capital efficiency, performance, market, and volatility timing of asian equity funds during COVID-19 outbreak, J. Asset Manag. 22 (2021), https://doi.org/10.1057/s41260-021-00228-y.
[7] G. Kavuran, SEM-Net: deep features selections with Binary Particle Swarm Optimization Method for classification of scanning electron microscope images, Mater Today Commun. 27 (2021), 102198, https://doi.org/10.1016/J.MTCOMM.2021.102198.
[8] G. Kavuran, When machine learning meets fractional-order chaotic signals: detecting dynamical variations, Chaos Solitons Fractals. 157 (2022), 111908, https://doi.org/10.1016/J.CHAOS.2022.111908.
[9] R. Vaishya, M. Javaid, I. Haleem, A. Haleem, Artificial Intelligence (AI) applications for COVID-19 pandemic Diabetes & Metabolic Syndrome : Clinical Research & Reviews Arti fi cial Intelligence (AI) applications for COVID-19 pandemic, Diabetes Metab. Syndr. 14 (2020).
[10] L. Li, L. Qin, Z. Xu, Y. Yin, X. Wang, B. Kong, J. Bai, Y. Lu, Z. Fang, Q. Song, K. Cao, D. Liu, G. Wang, Q. Xu, X. Fang, S. Zhang, J. Xia, J. Xia, Using artificial intelligence to detect COVID-19 and community-acquired pneumonia based on pulmonary CT: evaluation of the diagnostic accuracy, Radiology 296 (2020) E65–E71, https://doi.org/10.1148/radiol.2020200905.
[11] C. Zheng, X. Deng, Q. Fu, Q. Zhou, J. Feng, H. Ma, W. Liu, X. Wang, Deep learning-based detection for COVID-19 from chest CT using weak label, MedRxiv. (2020), https://doi.org/10.1101/2020.03.12.20027185.
[12] M. Loey, S. Mirjalili, COVID-19 cough sound symptoms classification from scalogram image representation using deep learning models, Comput Biol Med. 139 (2021), 105020, https://doi.org/10.1016/J.COMPBIOMED.2021.105020.

[13] Z. Liao, P. Lan, X. Fan, B. Kelly, A. Innes, Z. Liao, SIRVD-DL: A COVID-19 deep learning prediction model based on time-dependent SIRVD, Comput Biol Med. 138 (2021), 104868, https://doi.org/10.1016/J.COMPBIOMED.2021.104868.
[14] M. Pahar, M. Klopper, R. Warren, T. Niesler, COVID-19 detection in cough, breath and speech using deep transfer learning and bottleneck features, Comput Biol Med. 141 (2022), 105153, https://doi.org/10.1016/J.COMPBIOMED.2021.105153.
[15] X. Mei, H.C. Lee, K. yue Diao, M. Huang, B. Lin, C. Liu, Z. Xie, Y. Ma, P.M. Robson, M. Chung, A. Bernheim, V. Mani, C. Calcagno, K. Li, S. Li, H. Shan, J. Lv, T. Zhao, J. Xia, Q. Long, S. Steinberger, A. Jacobi, T. Deyer, M. Luksza, F. Liu, B.P. Little, Z.A. Fayad, Y. Yang, Artificial intelligence–enabled rapid diagnosis of patients with COVID-19, Nat. Med. 26 (2020), doi: 10.1038/s41591-020-0931-3.
[16] J. Laguarta, F. Hueto, B. Subirana, COVID-19 artificial intelligence diagnosis using only cough recordings, IEEE Open J Eng Med Biol. 1 (2020), https://doi.org/10.1109/ojemb.2020.3026928.
[17] S. Sakib, T. Tazrin, M.M. Fouda, Z.M. Fadlullah, M. Guizani, DL-CRC: Deep learning-based chest radiograph classification for covid-19 detection: a novel approach, IEEE Access 8 (2020), https://doi.org/10.1109/ACCESS.2020.3025010.
[18] A. Sedik, M. Hammad, F.E. Abd El-Samie, B.B. Gupta, A.A. Abd El-Latif, Efficient deep learning approach for augmented detection of Coronavirus disease, Neural Comput Appl. (2021), https://doi.org/10.1007/s00521-020-05410-8.
[19] M.F. Aslan, M.F. Unlersen, K. Sabanci, A. Durdu, CNN-based transfer learning–BiLSTM network: a novel approach for COVID-19 infection detection, Appl Soft Comput. 98 (2021), https://doi.org/10.1016/j.asoc.2020.106912.
[20] Y.H. Wu, S.H. Gao, J. Mei, J. Xu, D.P. Fan, R.G. Zhang, M.M. Cheng, JCS: an explainable COVID-19 diagnosis system by joint classification and segmentation, IEEE Trans. Image Process. 30 (2021), https://doi.org/10.1109/TIP.2021.3058783.
[21] K.U. Ahamed, M. Islam, A. Uddin, A. Akhter, B.K. Paul, M.A. Yousuf, S. Uddin, J.M. W. Quinn, M.A. Moni, A deep learning approach using effective preprocessing techniques to detect COVID-19 from chest CT-scan and X-ray images, Comput Biol Med. 139 (2021), 105014, https://doi.org/10.1016/J.COMPBIOMED.2021.105014.
[22] G. Kavuran, E. İn, A.A. Geçkil, M. Şahin, N.K. Berber, MTU-COVNet: a hybrid methodology for diagnosing the COVID-19 pneumonia with optimized features from multi-net, Clin Imaging. 81 (2022) 1–8, https://doi.org/10.1016/J.CLINIMAG.2021.09.007.
[23] E. Dong, H. Du, L. Gardner, An interactive web-based dashboard to track COVID-19 in real time, Lancet Infect Dis. 20 (2020) 533–534, accessed February 9, 2022.
[24] Human Development Index (HDI) | Human Development Reports, (n.d.). Available from: <https://hdr.undp.org/en/content/human-development-index-hdi> (accessed February 9, 2022).
[25] F.J. Ferri, P. Pudil, M. Hatef, J. Kittler, Comparative study of techniques for large-scale feature selection, Mach. Intelligence Pattern Recogn. (1994), https://doi.org/10.1016/B978-0-444-81892-8.50040-7.
[26] X. Hu, S. Yuan, F. Xu, Y. Leng, K. Yuan, Q. Yuan, Scalp EEG classification using deep Bi-LSTM network for seizure detection, Comput Biol Med. 124 (2020), 103919, https://doi.org/10.1016/j.compbiomed.2020.103919.
[27] D. Wang, Deep learning reinvents the hearing aid, IEEE Spectr. 54 (2017) 32–37, https://doi.org/10.1109/MSPEC.2017.7864754.
[28] C. Cortes, V. Vapnik, Support-vector networks, Mach Learn. (1995), https://doi.org/10.1023/A:1022627411411.
[29] V. Vapnik, The support vector method of function estimation, in: Nonlinear Modeling, Springer US, Boston, MA, 1998, pp. 55–85, doi: 10.1007/978-1-4615-5703-6_3.
[30] C.J.C. Burges, A tutorial on support vector machines for pattern recognition, Data Min Knowl Discov. 2 (1998) 121–167, https://doi.org/10.1023/A:1009715923555.
[31] A. Roghani, The relationship between macro-socioeconomics determinants and COVID-19 vaccine distribution, AIMS Public Health. 8 (2021) 655, https://doi.org/10.3934/PUBLICHEALTH.2021052.
[32] A. Ghosh, S. Nundy, T.K. Mallick, How India is dealing with COVID-19 pandemic, Sensors Int. 1 (2020), 100021, https://doi.org/10.1016/J.SINTL.2020.100021.
[33] M. Karmakar, P.M. Lantz, R. Tipirneni, Association of social and demographic factors With COVID-19 incidence and death rates in the US, JAMA Netw Open. 4 (2021), https://doi.org/10.1001/JAMANETWORKOPEN.2020.36462.
[34] Y. Qian, W. Fan, Who loses income during the COVID-19 outbreak? Evidence from China, Res. Soc. Stratif. Mobil. 68 (2020), 100522, https://doi.org/10.1016/J.RSSM.2020.100522.
[35] M.H. Heo, Y.D. Kwon, J. Cheon, K.B. Kim, J.W. Noh, Association between the human development index and confirmed COVID-19 cases by country, Healthcare (Basel) 10 (2022), https://doi.org/10.3390/HEALTHCARE10081417.
[36] C.V.C. Palamim, M.N. Boschiero, F.E. Valencise, F.A.L. Marson, Human development index is associated with COVID-19 case fatality rate in Brazil: an ecological study, Int. J. Environ. Res. Public Health 19 (2022) 5306, https://doi.org/10.3390/IJERPH19095306/S1.
[37] S.A. Ameye, T.O. Ojo, T.A. Adetunji, M.O. Awoleye, Is there an association between COVID-19 mortality and Human development index? The case study of Nigeria and some selected countries, BMC Res. Notes 15 (2022) 1–7, https://doi.org/10.1186/S13104-022-06070-8/FIGURES/3.